Electronic Supplementary Material (ESI) for Journal of Materials Chemistry C.

Supporting Information

Water content control during solution-based polymerization: a key to reach extremely high conductivity in PEDOT thin films

Amélie Schultheiss[#], Alexandre Carella[#], Stéphanie Pouget[§], Jérôme Faure-Vincent[§], Renaud Demadrille[§], Amélie Revaux[#], Jean-Pierre Simonato[#,ǂ]**

[#] University Grenoble Alpes, CEA/LITEN/DTNM, Grenoble, 38000, France
[§] University Grenoble Alpes, CEA/CNRS/IRIG, Grenoble, 38000, France
[ǂ] Department of Chemistry, Duke University, Durham, NC 27708, USA

Corresponding authors: jean-pierre.simonato@cea.fr; alexandre.carella@cea.fr

Table S1. Variations of synthesis conditions (temperature and humidity) and associated conductivities of PEDOT thin films. AA : ambient atmosphere ; AR : anhydrous room.

Entry	Atmosphere	Temperature	Resistance ($\Omega.\square^{-1}$)	Thickness (nm)	Conductivity ($S.cm^{-1}$)
1	AA	29°C	238 ± 19	46.5 ± 3.7	905 ± 142
2	AA	20°C	415 ± 27	24.3 ± 1.9	992 ± 140
3	Dry air flux	20°C	257 ± 4	16.7 ± 0.8	2330 ± 141
4	Argon flux	20°C	176 ± 6	22.2 ± 1.0	2560 ± 196
5	AR	23°C	159 ± 5	22.4 ± 1.9	2808 ± 224

Table S2. Water content in solutions determined by Karl-Fisher titration

	Water in EtOH (ppm)	Water in NMP (ppm)	Water in [EtOH + NMP] mixed solution (ppm)	Water - EDOT equivalent
Solvent + PEG-PPP-PEG	910	2100	1002	0.251
Dried solvant (72h)	50	120	55	0.014
Dried solvent (72h) + PEG-PPP-PEG	231	420	246	0.061

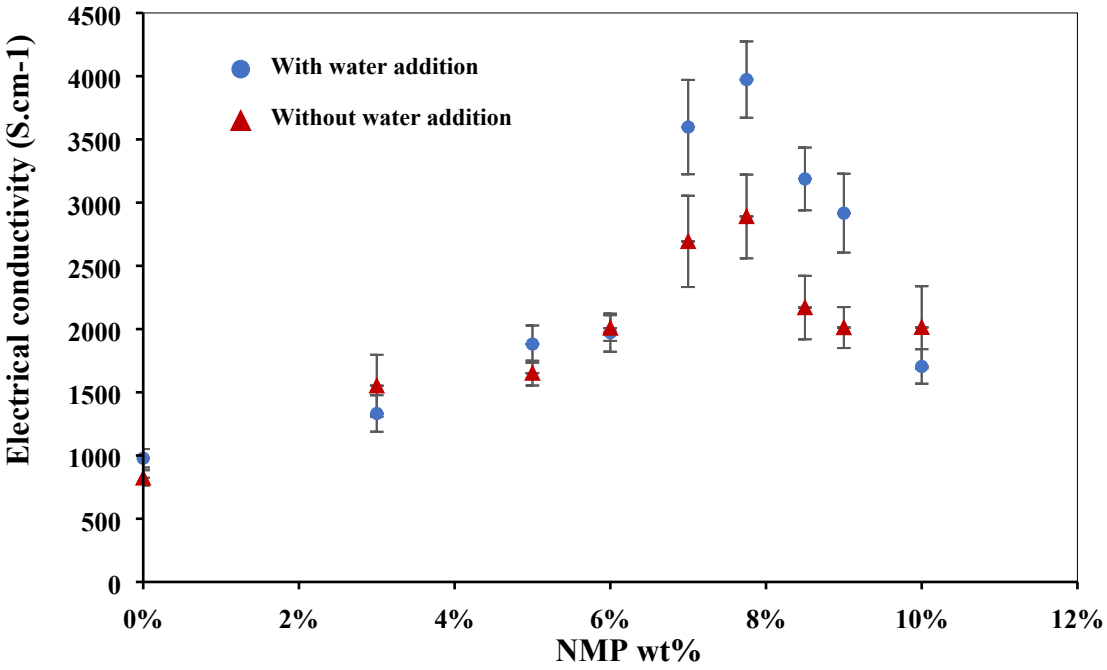

Figure S1. PEDOT:OTf conductivity of samples prepared in the anhydrous room, as a function of NMP content (wt%), with and without addition of H_2O (2 EDOT equivalents) in the oxidative solution

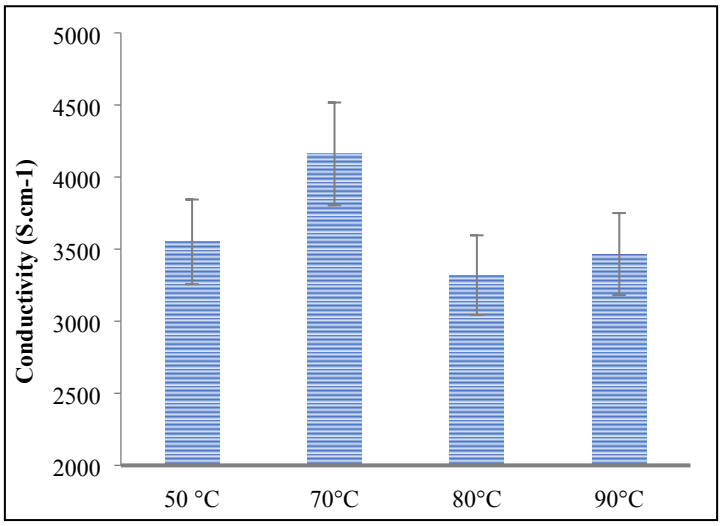

Figure S2. PEDOT:OTf conductivity of samples prepared in the anhydrous room with optimized water content (AR + 2 eq. H_2O), as a function of the annealing temperature.

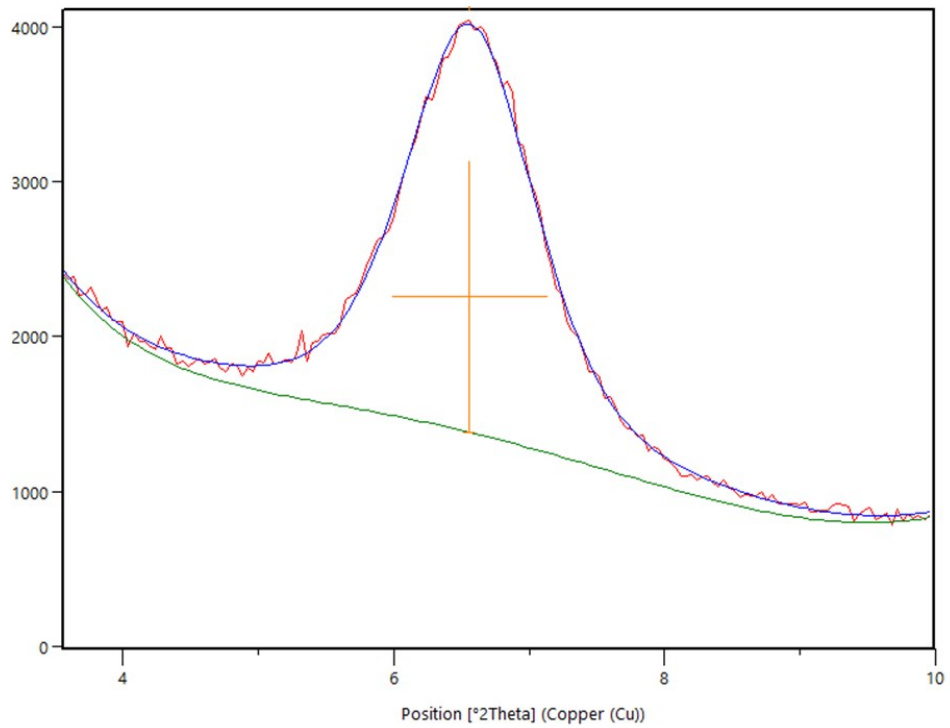

Figure S3. Theta/two-theta out-of-plane scan measured on PEDOT:OTf. The blue line corresponds to the result of the peak fitting with the sum of a pseudo-Voigt shape function and a background contribution (green line). The orange cross indicates the peak position and the FWHM. All the fits were performed keeping the value of the shape parameter of the pseudo-Voigt function constant at $\eta = 0.6$.

Table S3. Results obtained from the analysis of the GIWAXS data.

		Ambiant air (summer)			**Anhydrous room + 2 eq. H_2O**		
PEDOT:OTf Out-of-plane (lamellar stacking)	Order	1	2	3	1	2	3
	Peak position ($Å^{-1}$)	0.46 ± 0.01	0.90 ± 0.02	1.36 ± 0.02	0.46 ± 0.01	0.90 ± 0.02	1.36 ± 0.02
	d-spacing (Å)	13.5 ± 0.3			13.6 ± 0.3		
	Integrated intensity	996	309	77	4190	1121	248
	FWHM ($Å^{-1}$)	0.09	0.11	0.13	0.08	0.09	0.10
	Crystallite size (nm)	12 ± 1			12 ± 1		
	Strain ε	0.09			0.05		
PEDOT:OTf In-plane (π-stacking)	Peak position ($Å^{-1}$)	1.83 ± 0.01			1.83 ± 0.01		
	d-spacing (Å)	3.43 ± 0.02			3.43 ± 0.02		
	Intensity	262			398		
	FWHM ($Å^{-1}$)	0.14			0.14		
	Crystallite size min.(nm)	5.0 ± 0.5			5.0 ± 0.5		
PEDOT:Sulf Out-of-plane (lamellar stacking)	Order	1	2	3	1	2	3
	Peak position ($Å^{-1}$)	0.46 ± 0.01	0.90 ± 0.02	1.36 ± 0.02	0.46 ± 0.01	0.91 ± 0.02	1.37 ± 0.02
	d-spacing (Å)	13.5 ± 0.3			13.4 ± 0.3		
	Integrated intensity	2590	722	342	6139	1620	856
	FWHM ($Å^{-1}$)	0.08	0.09	0.12	0.08	0.09	0.11
	Crystallite size (nm)	14 ± 1			14 ± 1		
	Strain ε	0.08			0.08		
PEDOT:Sulf In-plane (π-stacking)	Peak position ($Å^{-1}$)	1.83 ± 0.01			1.84 ± 0.01		
	d-spacing (Å)	3.43 ± 0.02			3.42 ± 0.02		
	Intensity	140			182		
	FWHM ($Å^{-1}$)	0.13			0.12		
	Crystallite size min.(nm)	5.5 ± 0.5			6.0 ± 0.5		

The width of the diffraction peaks is related to the crystallite size (L) and the lattice distorsion (ε) by the following equation:

$$FW_{2\theta}(\theta) = \frac{K.\lambda}{L.cos(\theta)} + \varepsilon.tan(\theta)$$

With L the crystallite size along the direction of the diffusion vector, K the shape factor the value of which is close to 1, λ the wavelength, $FW_{2\theta}(\theta)$ the full width at half maximum, θ half of the scattering angle and ε the strain ($\varepsilon=4.\frac{<d-<d>>}{<d>}$).

The fit of several peaks corresponding to different orders of diffraction (here only the three first orders were used) allows the determination of both size and strain contributions, following the Williamson-Hall approach. For both samples the value of the lattice distorsion ε determined from the peaks associated to the lamellar stacking is of the order of 0.1%.

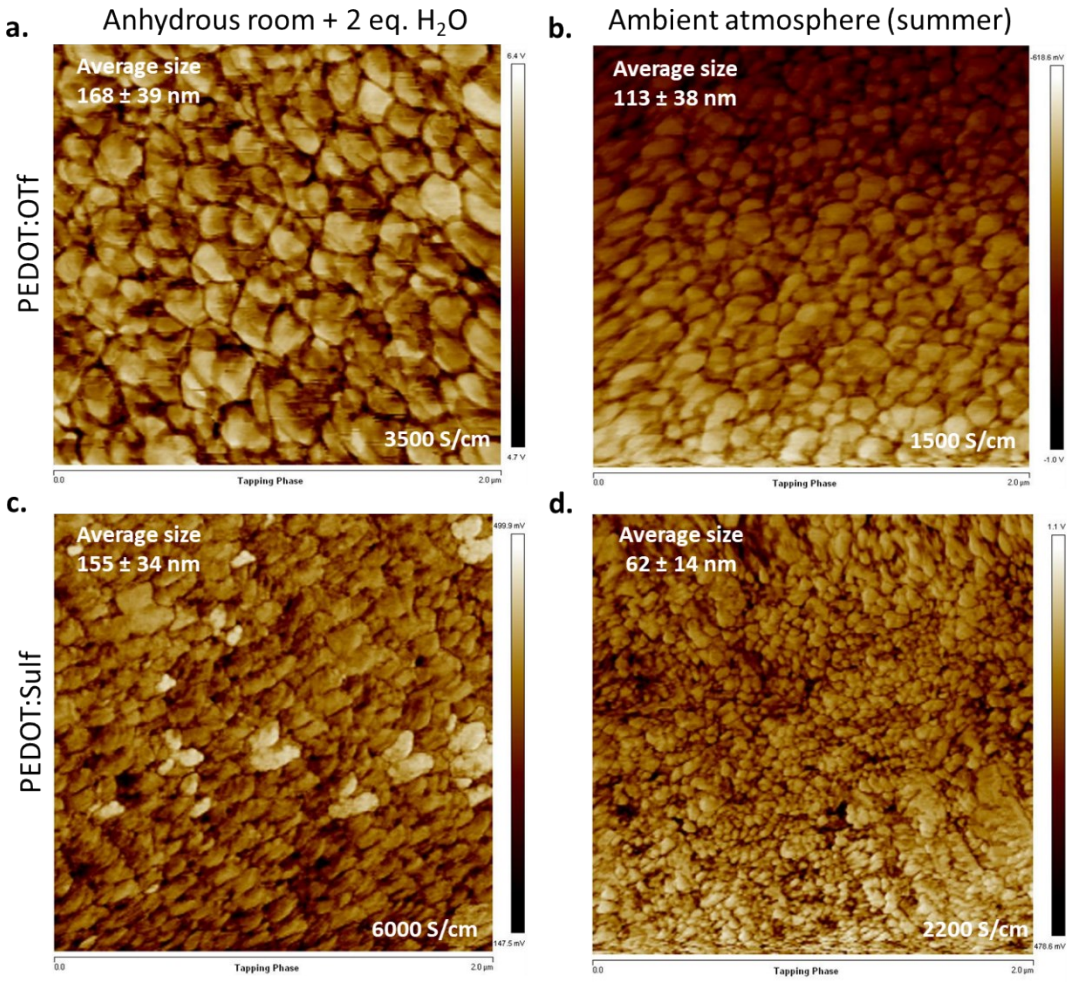

Figure S4. Phase AFM imaging (2x2 μm²) of PEDOT:OTf (a,b) and PEDOT:Sulf (c,d) for samples prepared in anhydrous room under optimized amount of water (a,c) and in summertime time at ambient atmosphere (b,d).

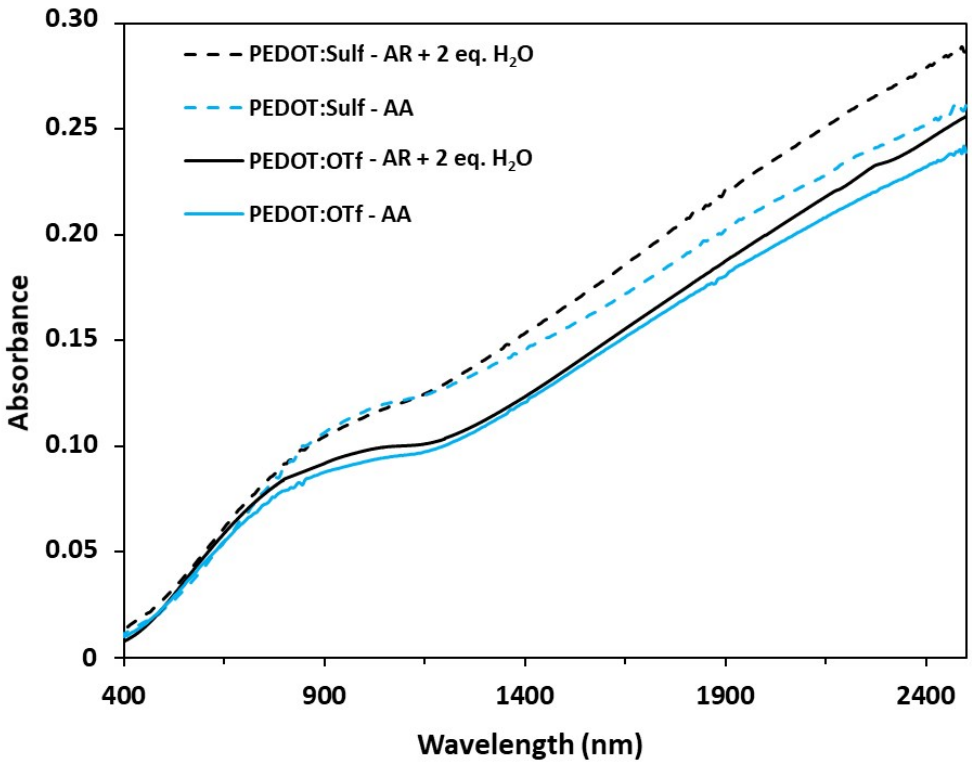

Figure S5. PEDOT:OTf and PEDOT:Sulf absorbance curves from 400 to 2500 nm, for samples prepared in summertime time at ambient atmosphere (AA) and in anhydrous room with optimized amount of water (AR + 2 eq. H_2O). Spectra were normalized to have similar absorbance at 400 nm.

Temperature dependent conductivity measurements

The temperature dependent conductivity curves were fitted with the following equations:

(1) Metal + (Sheng // Disordered metal):

$$\frac{\sigma(T)}{\sigma\,(300K)} = \left\{ Mexp\left(-\frac{T_m}{T}\right) + \left[\left(Nexp\left(\frac{T_1}{T+T_0}\right)\right)^{-1} + DM\right]^{-1}\right\}^{-1}$$

(2) Metal + (VRH // Disordered metal):

$$\frac{\sigma(T)}{\sigma\,(300K)} = \left\{ Mexp\left(-\frac{T_m}{T}\right) + \left[\left(V_0\exp\left(\left(\frac{T_{V0}}{T}\right)^{\frac{1}{n+1}}\right)\right)^{-1} + DM\right]^{-1}\right\}^{-1}$$

Table S4. Resistivity ratios and conduction contributions at 300 K, deduced from fitting parameters. The quasi 1D-metal resistivity contribution (%) is calculated for T=300 K, thanks to the quasi 1D-metal part (blue part) of the previous equations and the fitting parameters. The

Sheng (or VRH) and disordered conductivity contributions (%) are calculated thanks to previous equations respectively from the orange (or brown) part and green part.

Materials	Resistivity ratio	Quasi 1D-metal ($S.cm^{-1}$)	Amorphous region		Quasi-1D metal resistivity contribution (%)	Amorphous region	
			Sheng or VRH ($S.cm^{-1}$)	Disordered metal ($S.cm^{-1}$)		Sheng or VRH conductivity contribution (%)	Disordered metal conductivity contribution (%)
PEDOT:OTf AA	2.4	36849	375 (VRH)	428	3.1	46.7 (VRH)	53.3
PEDOT:OTf AR + $H_2O_{(2eq.)}$	1.6	85917	1848 (Sheng)	878	3.1	67.8 (Sheng)	32.2
PEDOT:Sulf AA	1.3	56186	1132 (Sheng)	2487	6.0	31.3 (Sheng)	68.7
PEDOT:Sulf AR + $H_2O_{(2eq.)}$	1.2	71842	1184 (Sheng)	3600	6.2	24.7 (Sheng)	75.3

Table S5. Fitting parameters of the heterogeneous models describing the conduction mechanism in the PEDOT films

Materials	M	T_m [K]	N	T_0 [K]	T_1 [K]	DM	V_0	T_{V0} [K]	n
PEDOT:OTf AA	37.3 ± 10.6	2124 ± 103	/	/	/	0.536 ±0.001	1.430 ± 0.005	136 ± 2	2 (fixed)
PEDOT:OTf AR + $H_2O_{(2eq.)}$	13 ± 9	1812 ± 222	1.26 ± 0.19	46 ± 6	46 ±5	0.330 ±0.004	/	/	/
PEDOT:Sulf AA	2.30 ± 0.11	1090 ± 17	2.55 ± 0.04	20.4 ± 0.9	53.2 ±0.3	0.730 ±0.004	/	/	/
PEDOT:Sulf AR + $H_2O_{(2eq.)}$	2.15 ± 0.08	1062 ± 15	3.17 ± 0.04	16.2 ± 0.8	56.7 ±0.6	0.800 ±0.002	/	/	/